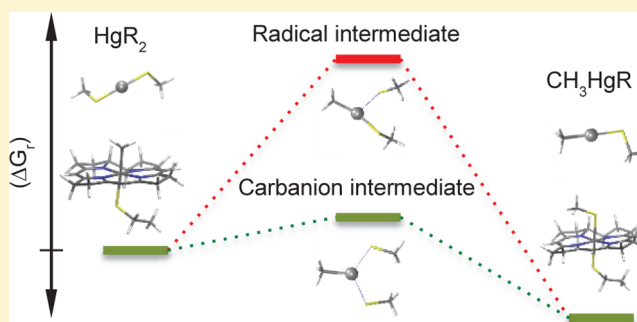


## Mercury Methylation by HgcA: Theory Supports Carbanion Transfer to Hg(II)

Jing Zhou,<sup>†,‡</sup> Demian Riccardi,<sup>‡</sup> Ariana Beste,<sup>§,||</sup> Jeremy C. Smith,<sup>‡,¶</sup> and Jerry M. Parks<sup>\*,‡</sup><sup>†</sup>Graduate School of Genome Science and Technology, University of Tennessee, Knoxville, Tennessee 37996, United States<sup>‡</sup>UT/ORNL Center for Molecular Biophysics, Oak Ridge National Laboratory, Oak Ridge, Tennessee 37831-6309, United States<sup>§</sup>Joint Institute for Computational Sciences, University of Tennessee, Oak Ridge, Tennessee 37831-6164, United States<sup>||</sup>Center for Nanophase Materials Science, Oak Ridge National Laboratory, Oak Ridge, Tennessee 37831, United States<sup>¶</sup>Department of Biochemistry and Cellular and Molecular Biology, University of Tennessee, Knoxville, Tennessee 37996, United States

## Supporting Information

**ABSTRACT:** Many proteins use corrinoid cofactors to facilitate methyl transfer reactions. Recently, a corrinoid protein, HgcA, has been shown to be required for the production of the neurotoxin methylmercury by anaerobic bacteria. A strictly conserved Cys residue in HgcA was predicted to be a lower-axial ligand to Co(III), which has never been observed in a corrinoid protein. Here, we use density functional theory to study homolytic and heterolytic Co–C bond dissociation and methyl transfer to Hg(II) substrates with model methylcobalamin complexes containing a lower-axial Cys or His ligand to cobalt, the latter of which is commonly found in other corrinoid proteins. We find that Cys thiolate coordination to Co facilitates both methyl radical and methyl carbanion transfer to Hg(II) substrates, but carbanion transfer is more favorable overall in the condensed phase. Thus, our findings are consistent with HgcA representing a new class of corrinoid protein capable of transferring methyl groups to electrophilic substrates.



## INTRODUCTION

Methylmercury ( $[\text{CH}_3\text{Hg}(\text{II})]^+$ ) is a potent neurotoxin that is produced in the environment from inorganic Hg.<sup>1</sup> It has been known for more than four decades that anaerobic microorganisms produce methylmercury from inorganic Hg(II).<sup>2,3</sup> Two decades ago, a corrinoid, i.e., cobalamin-dependent, protein associated with the acetyl-CoA biochemical pathway was shown to be responsible for methylmercury production in the anaerobic bacterium *Desulfovibrio desulfuricans* LS,<sup>4</sup> but the protein was not characterized further. In later work, on the basis of acetyl CoA pathway inhibition<sup>5</sup> and cobalt limitation<sup>6</sup> studies, it was proposed that microorganisms lacking the complete acetyl-CoA pathway produce methylmercury through an alternate, cobalamin-independent pathway. Recently, it was shown that two genes, *hgcA* and *hgcB*, are required for methylmercury production by the model methylating sulfate-reducing bacterium *Desulfovibrio desulfuricans* ND132<sup>7</sup> and the iron-reducing bacterium *Geobacter sulfurreducens* PCA.<sup>8</sup> These genes encode a corrinoid protein, HgcA, and an auxiliary 2[4Fe-4S] ferredoxin-like protein, HgcB, and the deletion of either gene abolished the ability of these organisms to produce methylmercury.<sup>8</sup> The *hgcAB* gene pair has been found in a diverse set of microorganisms from bacterial and archaeal phyla, including the *Proteobacteria*, *Firmicutes*, *Chloroflexi*, and

*Euryarchaeota*. Outside the *Deltaproteobacteria*, none of these microorganisms had been tested previously for their ability to methylate mercury, but the predicted mercury methylation phenotype for organisms possessing *hgcAB* has subsequently been confirmed for all organisms tested to date.<sup>9,10</sup>

Corrinoid proteins use cobalamin or related cofactors to facilitate many types of reactions, including methyl transfer.<sup>11–13</sup> In principle, methylcob(III)alamin can transfer a methyl group as a carbocation ( $\text{CH}_3^+$ ), radical ( $\text{CH}_3^\bullet$ ), or carbanion ( $\text{CH}_3^-$ ).<sup>12,14,15</sup> The particular type of methyl transfer that is carried out by a given corrinoid protein depends in part on the lower-axial ligand to the Co center of the cofactor. However, all cobalamin-dependent methyltransferases characterized so far have been found to transfer carbocations.<sup>16</sup>

Protein sequence analysis and homology modeling of HgcA from *D. desulfuricans* ND132 using an X-ray structure of the corrinoid iron–sulfur protein from *Carboxydotherrmus hydrogeniformans* Z-2901<sup>17</sup> as a template suggested that the 5,6-dimethylbenzimidazole (DMB) tail of the cofactor is not coordinated to Co (i.e., “DMB-off”), but a strictly conserved Cys residue in HgcA may be the lower-axial ligand to Co

Received: August 1, 2013

Published: December 30, 2013

instead. UV–visible spectra were consistent with this mode of coordination, although they were not fully conclusive.<sup>8</sup>

Methylcobalamin is known to methylate inorganic Hg(II) to produce methylmercury nonenzymatically,<sup>18,19</sup> and coordination of Co by the DMB tail promotes this reaction<sup>14,20</sup> However, a thiolate ligand would be expected to coordinate strongly with CH<sub>3</sub>–cob(III)alamin if the DMB tail is absent or displaced. Thiolate-induced reductive cleavage of the Co–C bond in methylcobalamin and methylcobinamide to generate species with carbanionic character was proposed in the context of acetate and methane synthesis,<sup>21,22</sup> but, to our knowledge, not in the context of Hg methylation. Nevertheless, methylmercury formation by HgcA may involve the transfer of a carbanion to a Hg(II) substrate, with the Cys thiolate ligand playing a key role in stabilizing the Co(III) state during the reaction (Figure 1). Because methylation of the cofactor is

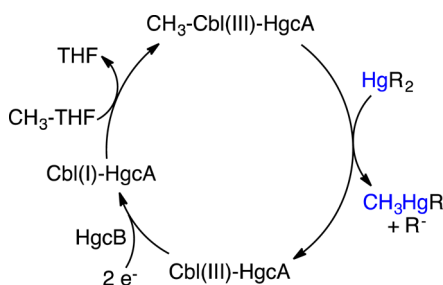
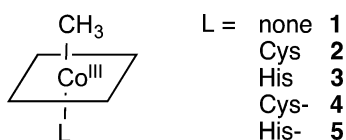


**Figure 1.** Proposed Hg methylation pathway adapted from ref 8. CH<sub>3</sub>–THF = 5-methyltetrahydrofolate, Cbl = cobalamin.

presumed to involve initial transfer of a carboxylation to a reduced Co(I) center followed by subsequent carbanion transfer to Hg(II), the cofactor in HgcA has been proposed to cycle between the Co(I), CH<sub>3</sub>–Co(III), and Co(III) states. Reduction of Co(III) back to the Co(I) state is then presumably carried out by HgcB.

Previous theoretical studies of methylcobalamins have focused on various aspects of Co–C homolysis,<sup>23–34</sup> and spectral and electronic properties.<sup>35–44</sup> To our knowledge, only two studies have investigated carbanion dissociation in models of methylcobalamin,<sup>38,45</sup> and none has considered the possible role of a lower-axial Cys thiolate ligand in promoting Co–C heterolysis. Here, we perform density functional theory calculations with empirical dispersion corrections to investigate whether a hypothetical lower-axial Cys thiolate ligand to Co could indeed facilitate methyl carbanion transfer to Hg(II) substrates. We represent cobalamin by corrin (C<sub>19</sub>H<sub>21</sub>N<sub>4</sub>Co). That is, the side chains and DMB tail have been replaced by hydrogen, which is a common approach for studying cobalamins. The lower-axial ligand is represented by a Cys or His side chain in either its neutral or anionic protonation state (Scheme 1). We first compute both homolytic and heterolytic bond dissociation energies (BDEs) of the Co–C bond in models of methylcob(III)alamin with different lower-axial

#### Scheme 1. Methylcorrinoid Model Systems with Various Lower-Axial Ligands



ligands, which allows direct comparison with previous studies. We then compute reaction free energies in the gaseous and condensed phases for methyl radical and carbanion transfer to two Hg(II) substrates. Finally, we compute ligand exchange free energies in which the methyl group bound to Co(III) is replaced with the leaving group from the Hg(II) substrate complex. Methyl carbocation dissociation and transfer reactions are not considered here because Hg–C bond formation between Hg(II) and CH<sub>3</sub><sup>+</sup> is not possible.

#### COMPUTATIONAL METHODS

All calculations were performed with NWChem<sup>46</sup> or Gaussian 09<sup>47</sup> using the BP86<sup>48–50</sup> functional, which was shown to yield homolytic Co–C BDEs for cobalamins in good agreement with experimental measurements.<sup>28</sup> The procedure used here to compute bond dissociation energies was similar to previous studies.<sup>25,26,28,51</sup> We include empirical dispersion corrections, which have been shown to provide improved accuracy for density functional theory calculations. BP86-D slightly overbinds the methyl group relative to experimental values for methylcobalamin,<sup>52</sup> but these errors should largely cancel for the relative energetics of interest here. Cob(III)alamin and cob(II)alamin are low-spin *d*<sub>6</sub> and *d*<sub>7</sub> complexes, respectively, and it has been shown that the low-spin Co(III)–corrin–ligand and Co(II)–corrin–ligand models of the type considered here are the lowest in energy.<sup>31</sup> Thus, all Co(III) and Co(II) complexes were assigned spin multiplicities of 1 and 2, respectively.

All geometries were fully optimized in the gas phase using “tight” convergence criteria as defined in NWChem. The “grid=xfine” option in NWChem was used for integral evaluation in all calculations. For geometry optimizations, the Stuttgart-Dresden small-core effective core potential (ECP), also called SDD or ECP60MWB, which accounts for scalar relativistic effects, and its corresponding basis set,<sup>53</sup> were used for Hg, and the 6-31G(d) basis set with spherical *d* functions was used for all other atoms. The SDD ECP has been used previously in conjunction with hybrid DFT to describe the Hg–C bond cleavage reaction catalyzed by the organomercurial lyase,<sup>54</sup> Hg(II) solvation<sup>55</sup> and Hg(II) ligand binding,<sup>36</sup> and with the BP86 functional to describe Hg(II) complexation with a porphyrin.<sup>57</sup>

Vibrational frequency analysis was performed for the fully optimized geometries to confirm that they were energy minima and to compute zero-point energy (ZPE) and thermal corrections. Vibrational frequencies were calculated analytically for closed-shell molecules and numerically for open-shell molecules with NWChem. Although the convergence criteria for the geometry optimizations were set to “tight”, the Co(II)–corrin complex produced a spurious imaginary frequency (25.38i cm<sup>–1</sup>) caused by inaccuracies in the numerical Hessian. Displacements along the spurious imaginary mode confirmed that the structure is indeed a minimum along this mode (Figure S1, Supporting Information, SI).

Single-point energies were computed at the optimized geometries with the SDD ECP and basis set for Hg and the 6-311++G(d,p) basis set for all other atoms. For simplicity, we refer to the 6-31G(d) and 6-311++G(d,p) basis sets as B1 and B2, respectively, with SDD being implied when Hg is present in the calculations. Empirical dispersion corrections<sup>58</sup> with Becke–Johnson damping,<sup>59</sup> (abbreviated as D3) were computed with the program DFT-D3<sup>60</sup> on geometries optimized with B1. Solvation effects were computed at gas-phase geometries with B1 using the SMD continuum solvation model<sup>61</sup> as implemented in Gaussian 09 with the default dielectric constant,  $\epsilon = 78.4$ , and with  $\epsilon = 4.0$ .

Gas-phase Co–C bond dissociation energies were computed as follows:

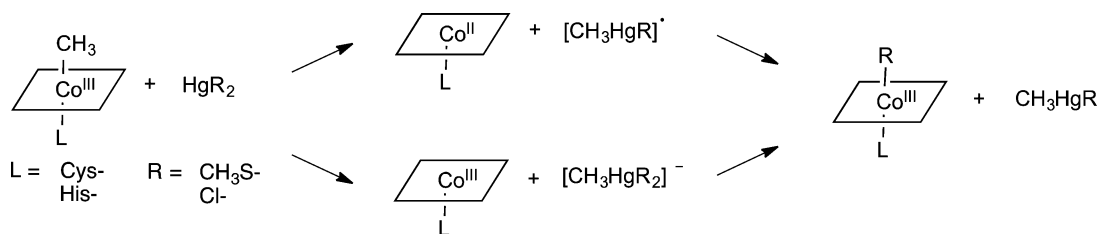
$$\text{BDE} = \Delta E_{\text{B2}} + \Delta E_{\text{ZPE,B1}} + \Delta E_{\text{disp}} + \Delta E_{\text{BSSE,B2}}$$

where  $\Delta E_{\text{B2}}$  is the difference in DFT total energy (products minus reactant) computed with B2,  $\Delta E_{\text{ZPE,B1}}$  is the zero-point energy correction obtained from vibrational frequency analysis computed with

**Table 1.** Computed Absolute and Relative<sup>a</sup> Gas-Phase Bond Dissociation Energies and Condensed Phase Reaction Free Energies (kcal mol<sup>-1</sup>) for Co–C Bond Dissociation in CH<sub>3</sub>–Co(III)–Corrin–Ligand Complexes

reaction	abs. BDE	rel. BDE	abs. $\Delta G_{r,\text{gas}}^\circ$	rel. $\Delta G_{r,\text{gas}}^\circ$	abs. $\Delta G_{r,\text{aq}}^{*\text{b}}$	rel. $\Delta G_{r,\text{aq}}^{*\text{b}}$
homolysis						
1	42.6	6.6	37.4	7.7	36.8 (38.7)	5.9 (6.8)
2	36.0	0.0	29.7	0	30.9 (31.9)	0.0 (0.0)
3	38.7	2.7	29.2	-0.5	30.9 (31.6)	0.0 (-0.3)
4	36.2	0.0	26.7	0	28.5 (29.3)	0.0 (0.0)
5	39.8	3.6	29.3	2.6	30.2 (31.5)	1.7 (2.2)
heterolysis						
1	275.1	36.3	269.1	34.6	80.9 (127.3)	31.2 (31.3)
2	238.8	0.0	234.5	0	49.7 (96.0)	0.0 (0.0)
3	234.6	-4.2	229.7	-4.8	47.8 (92.6)	-1.9 (-3.4)
4	141.2	0.0	135.8	0	26.4 (53.2)	0.0 (0.0)
5	155.6	14.4	149.7	13.9	38.5 (66.4)	12.1(13.2)

<sup>a</sup>Relative to the Cys ligand complex (2 or 4) within each charge/dissociation category. <sup>b</sup> $\epsilon = 78.4$  ( $\epsilon = 4.0$ ). See text.

**Scheme 2.** Methyl Transfer to Hg(SCH<sub>3</sub>)<sub>2</sub> and HgCl<sub>2</sub> with Subsequent Ligand Exchange

B1,  $\Delta E_{\text{disp}}$  is the dispersion correction, and  $\Delta E_{\text{BSE}}$  is the standard counterpoise correction<sup>62</sup> computed with B2.

Gas-phase reaction free energies at 298.15 K and 1 atm ( $\Delta G_{r,\text{gas}}^\circ$ ) were computed for all processes as follows:

$$\Delta G_{r,\text{gas}}^\circ = \Delta E_{\text{B2}} + \Delta E_{\text{disp}} + \Delta H_{\text{corr},\text{B1}}^\circ - T\Delta S_{\text{corr},\text{B1}}^\circ$$

where the first two terms on the RHS are the same as for the BDEs,  $\Delta H_{\text{corr},\text{B1}}^\circ$  and  $T\Delta S_{\text{corr},\text{B1}}^\circ$  are the thermal corrections to the enthalpy and entropy, respectively, computed with the standard ideal gas, rigid-rotor, harmonic approximation.

Aqueous phase reaction free energies at 298.15 K and 1 M ( $\Delta G_{r,\text{aq}}^{*\text{b}}$ ) were computed for all processes as:

$$\Delta G_{r,\text{aq}}^{*\text{b}} = \Delta G_{r,\text{gas}}^\circ + \Delta \Delta G_{\text{solv},\text{B1}}^{\circ \rightarrow *}$$

where  $\Delta \Delta G_{\text{solv},\text{B1}}^{\circ \rightarrow *}$  is the solvation free energy difference for the reaction computed with the SMD continuum solvent model. The individual solvation free energies for each solute include a contribution ( $\Delta G^{\circ \rightarrow *} = 1.89$  kcal mol<sup>-1</sup>) arising from changing the standard state from 1 mol per 24.46 L in the gas phase to 1 M in the condensed phase.

## RESULTS AND DISCUSSION

**Co–C Bond Homolysis.** The computed gas-phase homolytic Co–C BDEs are all in the range of ~36–43 kcal mol<sup>-1</sup> (Table 1), consistent with previous studies.<sup>23–26,28,31–33</sup>

For heterolytic Co–C dissociation, the BDEs are of course much higher in the gas phase than for homolysis because of charge separation in the heterolytically dissociated fragments (Table 1). To enable direct comparisons of homolytic and heterolytic processes, we computed reaction free energies for Co–C bond dissociation with a continuum representation of the solvent.

For methyl radical dissociation in the gas phase, the computed Co–C BDE with a neutral Cys ligand (2) is 2.7 kcal mol<sup>-1</sup> lower than for the neutral His ligand complex (3) (Table 1). Similarly, the computed homolytic BDE for the Cys

thiolate complex (4) is 3.6 kcal mol<sup>-1</sup> lower than for the His imidazolate complex (5) (Table 1). These findings are consistent with a previous study that showed that lower-axial Co coordination by sulfides yielded the lowest homolytic BDEs among a series of small molecule and amino-acid side chain ligand models.<sup>31</sup> Homolytic dissociation in the absence of a lower-axial ligand (1) was computed to be 6.6 kcal mol<sup>-1</sup> less favorable than for the Cys-coordinated complex (2) (Table 1). We computed gas-phase reaction free energies ( $\Delta G_{r,\text{gas}}^\circ$ ) for each process and found that the sum of the enthalpic (-3.3 to -4.5 kcal mol<sup>-1</sup>) and entropic contributions (7.2 to 12.9 kcal mol<sup>-1</sup>) provided net stabilization of the products relative to the corresponding BDE values. We also computed aqueous phase reaction free energies ( $\Delta G_{r,\text{aq}}^{*\text{b}}$ ) by including solvation contributions obtained with the Solvent Model based on Density<sup>61</sup> (SMD) polarizable continuum model and the dielectric constant of water (SMD<sub>78.4</sub>). Solvation effects were generally slightly destabilizing for radical transfer (<2 kcal mol<sup>-1</sup>) relative to the gas-phase reaction free energies (Table 1).

**Co–C Bond Heterolysis.** For methyl carbanion dissociation, the computed heterolytic BDE for the CH<sub>3</sub>–Co(III)–corrin complex with a neutral Cys ligand (2) is 4.2 kcal mol<sup>-1</sup> less favorable than for the neutral His ligand complex (3) (Table 1) because the neutral Cys side chain interacts more weakly than neutral His with Co(III). In the absence of a lower-axial ligand, heterolytic dissociation (1) is much less favorable (by more than 36 kcal mol<sup>-1</sup> in the gas phase and ~31 kcal mol<sup>-1</sup> in water) than for the Cys or His ligand complexes. Indeed, five-coordinate, “base-off” CH<sub>3</sub>–cob(III)alamin in corrinoid proteins is known to favor methyl carbocation transfer.<sup>11,12,45,63</sup> However, the heterolytic Co–C dissociation of the Cys thiolate complex (4) is 14.4 kcal mol<sup>-1</sup> more favorable than for the His imidazolate complex (5). Similar to the homolytic processes, the sum of the enthalpic (-3.7 to

**Table 2.** Computed Gas-Phase and Aqueous Reaction Free Energies for Methyl Radical and Carbanion Transfer from CH<sub>3</sub>-Co(III)-Corrin-Ligand Complexes to Hg(SCH<sub>3</sub>)<sub>2</sub> and HgCl<sub>2</sub>

	reaction	$\Delta G^\circ_{r,\text{gas}}$	$\Delta G^*_{r,\text{aq}}^a$
A	CH <sub>3</sub> -Co(III)-corrin-Cys(-) + Hg(SCH <sub>3</sub> ) <sub>2</sub> → Co(II)-corrin-Cys(-) + [CH <sub>3</sub> Hg(SCH <sub>3</sub> ) <sub>2</sub> ] <sup>•</sup>	23.3	27.4 (26.6)
B	CH <sub>3</sub> -Co(III)-corrin-His(-) + Hg(SCH <sub>3</sub> ) <sub>2</sub> → Co(II)-corrin-His(-) + [CH <sub>3</sub> Hg(SCH <sub>3</sub> ) <sub>2</sub> ] <sup>•</sup>	26.0	29.2 (28.8)
C	CH <sub>3</sub> -Co(III)-corrin-Cys(-) + HgCl <sub>2</sub> → Co(II)-corrin-Cys(-) + [CH <sub>3</sub> HgCl <sub>2</sub> ] <sup>•</sup>	26.5	29.7 (29.1)
D	CH <sub>3</sub> -Co(III)-corrin-His(-) + HgCl <sub>2</sub> → Co(II)-corrin-His(-) + [CH <sub>3</sub> HgCl <sub>2</sub> ] <sup>•</sup>	29.1	31.4 (31.3)
E	CH <sub>3</sub> -Co(III)-corrin-Cys(-) + Hg(SCH <sub>3</sub> ) <sub>2</sub> → Co(III)-corrin-Cys(-) + [CH <sub>3</sub> Hg(SCH <sub>3</sub> ) <sub>2</sub> ] <sup>-</sup>	69.9	5.1 (19.1)
F	CH <sub>3</sub> -Co(III)-corrin-His(-) + Hg(SCH <sub>3</sub> ) <sub>2</sub> → Co(III)-corrin-His(-) + [CH <sub>3</sub> Hg(SCH <sub>3</sub> ) <sub>2</sub> ] <sup>-</sup>	83.8	17.1 (32.3)
G	CH <sub>3</sub> -Co(III)-corrin-Cys(-) + HgCl <sub>2</sub> → Co(III)-corrin-Cys(-) + [CH <sub>3</sub> HgCl <sub>2</sub> ] <sup>-</sup>	46.5	-16.0 (-3.8)
H	CH <sub>3</sub> -Co(III)-corrin-His(-) + HgCl <sub>2</sub> → Co(III)-corrin-His(-) + [CH <sub>3</sub> HgCl <sub>2</sub> ] <sup>-</sup>	60.4	-4.0 (9.4)

<sup>a</sup> $\epsilon = 78.4$  ( $\epsilon = 4.0$ ).

-6.1 kcal mol<sup>-1</sup>) and entropic contributions (8.6 to 11.3 kcal mol<sup>-1</sup>) provided net stabilization of the products relative to the corresponding BDE values, with heterolytic dissociation of **4** remaining ~14 kcal mol<sup>-1</sup> more favorable than for **5**. Solvation stabilizes the charges of the dissociated species for heterolytic Co-C cleavage of **1-5** and greatly reduces their respective reaction free energies relative to the gas phase (Table 1). In the aqueous phase (SMD<sub>78.4</sub>), dissociation of a carbanion for the Cys-on species (**4**) requires the least energy (26.4 kcal mol<sup>-1</sup>) compared to all other homolytic and heterolytic dissociation processes. However, homolysis becomes more favorable (by 14–24 kcal mol<sup>-1</sup>) when the dielectric constant is lowered to approximate a protein environment (SMD<sub>4.0</sub>).

**Reaction Free Energies.** To compare methyl radical and carbanion transfer to Hg(II) in the condensed phase, we computed aqueous reaction free energies for both types of transfer from CH<sub>3</sub>-Co(III)-corrin-ligand complexes to two Hg(II) substrates (Scheme 2). Hg(II) bis thiolates, which were modeled as Hg(SCH<sub>3</sub>)<sub>2</sub>, were found to be the most prevalent form of Hg inside the cells of *D. desulfuricans* ND132.<sup>64</sup> We also consider HgCl<sub>2</sub> as a substrate because it is readily methylated under aqueous, nonenzymatic conditions. In metalloproteins, endogenous protic acid ligands typically coordinate metal centers as anions,<sup>65</sup> so we limit these analysis to complexes with a Cys or His ligand in the anionic protonation state (i.e., **4** and **5**).

Similar to the trends observed for the gas-phase reaction free energies for Co-C bond dissociation, methyl radical transfer to Hg(SCH<sub>3</sub>)<sub>2</sub> was computed to be 2.7 kcal mol<sup>-1</sup> more favorable for the complex with a Cys(-) ligand (Reaction A) than for His(-) (Reaction B, Table 2). Methyl radical transfer to HgCl<sub>2</sub> is also favored for the Cys(-) complex (Reaction C) over the His(-) complex (Reaction D) by a similar amount. Including solvation (SMD<sub>78.4</sub> and SMD<sub>4.0</sub>) slightly increases the reaction free energies ( $\Delta G^*_{r,\text{aq}}$ ) for methyl radical transfer by ~2–4 kcal mol<sup>-1</sup> relative to the gas phase. Comparing the gas-phase bond dissociation free energies (Table 1) to Reactions A through D (Table 2) reveals that the Hg-C interactions in the methylated Hg(II) complexes do not significantly enhance homolytic transfer.

Methyl carbanion transfer to both Hg(SCH<sub>3</sub>)<sub>2</sub> and HgCl<sub>2</sub> were computed to be ~14 kcal mol<sup>-1</sup> more favorable in the gas phase for the Cys(-) complex (Reactions E and G, respectively) compared with the corresponding His(-) complex (Reactions F and H, respectively) (Table 2). Methyl carbanion transfer to HgCl<sub>2</sub> (Reactions G and H) is ~23 kcal mol<sup>-1</sup> more favorable in the gas phase than to Hg(SCH<sub>3</sub>)<sub>2</sub> (Reactions E and F) for both Cys(-) and His(-) ligand complexes (Table 2), consistent with the greater reactivity of

Hg(II) in HgCl<sub>2</sub>.<sup>56</sup> Solvation lowers the reaction free energies for methyl carbanion transfer drastically relative to the corresponding processes in the gas phase. The aqueous phase reaction free energy for carbanion transfer from Cys(-) complex **4** to Hg(SCH<sub>3</sub>)<sub>2</sub> (Reaction E) was computed to be 5.1 kcal mol<sup>-1</sup>, ~12 kcal mol<sup>-1</sup> more favorable than for His(-) complex **5** (Reaction F). Reactions G and H were both computed to be exergonic (Table 2), with carbanion transfer to HgCl<sub>2</sub> being ~12 kcal mol<sup>-1</sup> more favorable for the Cys(-) complex (**4**) than for the His(-) complex (**5**). Compared to aqueous conditions (SMD<sub>78.4</sub>), these reactions (E-H) were computed to be 12–15 kcal mol<sup>-1</sup> less favorable in the approximated protein environment (SMD<sub>4.0</sub>). Nevertheless, when condensed phase effects are included, methyl carbanion transfer from Cys(-) complex **4** is still favored over His(-) complex **5** for both Hg(II) substrates. Perhaps more importantly, methyl carbanion transfer to Hg(II) substrates is significantly more favorable overall than methyl radical transfer (Table 2 and Figure 2). In contrast to methyl radical transfer to Hg(II) substrates, the Hg-C interactions in the [CH<sub>3</sub>HgR<sub>2</sub>]<sup>-</sup> complexes significantly enhance heterolytic transfer.

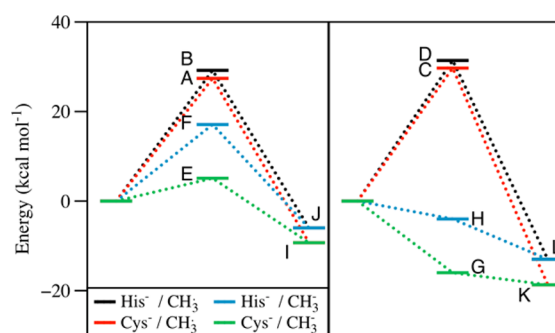


**Figure 2.** Aqueous reaction free energies ( $\Delta G^*_{r,\text{aq}}$ ) relative to reactants for methyl radical and carbanion transfer (Reactions A–H), and ligand exchange free energies (Reactions I–L). (Left) Hg(SCH<sub>3</sub>)<sub>2</sub> substrate, (right) HgCl<sub>2</sub> substrate. See Scheme 2 for details.

**Nonenzymatic Hg Methylation.** The present findings are also relevant to the nonenzymatic methylation of Hg(II) by methylcobalamin,<sup>18,19</sup> which is known to be enhanced by coordination of the DMB tail to Co.<sup>14,20</sup> The DMB tail has only one nitrogen available for Co coordination because the second is bonded to the ribofuranosyl moiety through an N-alkyl linkage. Thus, the neutral His (i.e., imidazole) complex (**3**) is the most relevant ligand for comparison. Indeed, substitution of DMB by imidazole in previous computational studies was

**Table 3. Computed Condensed-Phase Reaction Free Energies<sup>a</sup> for Upper-Axial Ligand Exchange in Co(III)–Corrin–Ligand Complexes**

	reaction	$\Delta G_{\text{r, gas}}^{\circ}$	$\Delta G_{\text{r, aq}}^{*b}$
I	$\text{CH}_3\text{-Co(III)-corrin-Cys(-)} + \text{Hg}(\text{SCH}_3)_2 \rightarrow \text{CH}_3\text{S-Co(III)-corrin-Cys(-)} + \text{CH}_3\text{HgSCH}_3$	-11.3	-9.3 (-10.7)
J	$\text{CH}_3\text{-Co(III)-corrin-His(-)} + \text{Hg}(\text{SCH}_3)_2 \rightarrow \text{CH}_3\text{S-Co(III)-corrin-His(-)} + \text{CH}_3\text{HgSCH}_3$	-7.8	-6.0 (-7.1)
K	$\text{CH}_3\text{-Co(III)-corrin-Cys(-)} + \text{HgCl}_2 \rightarrow \text{Cl-Co(III)-corrin-Cys(-)} + \text{CH}_3\text{HgCl}$	-21.2	-18.7 (-20.0)
L	$\text{CH}_3\text{-Co(III)-corrin-His(-)} + \text{HgCl}_2 \rightarrow \text{Cl-Co(III)-corrin-His(-)} + \text{CH}_3\text{HgCl}$	-16.9	-13.0 (-14.7)

<sup>a</sup>See Methods and SI for details. <sup>b</sup> $\epsilon = 78.4$  ( $\epsilon = 4.0$ ). See text.

shown to yield good accuracy for computing Co–C strengths.<sup>23,32,66–68</sup> Using the SMD<sub>78.4</sub> bond dissociation free energies from Table 1, transfer of a carbanion from 3 to HgCl<sub>2</sub> increases the reaction energy from -4.0 kcal mol<sup>-1</sup> (Reaction H) to 5.3 kcal mol<sup>-1</sup> relative to 5. Thus, the present calculations suggest that methyl carbanion transfer from methylcobalamin to HgCl<sub>2</sub> is energetically feasible for methylcobalamin in the DMB-on configuration in the aqueous phase. In contrast, for SMD<sub>4.0</sub> the corresponding substitution of the neutral imidazole for imidazolate increases the energetic cost from 9.4 (Reaction H) to 35.6 kcal mol<sup>-1</sup>. Apparently, swapping an anionic ligand for the DMB tail is necessary to achieve reasonable energetics in the protein environment for methyl transfer to an electrophilic substrate.

**Ligand Exchange Reactions.** In an aqueous environment,  $[\text{CH}_3\text{Hg(II)R}_2]^{n-}$  ( $\text{R} = \text{CH}_3\text{S}^-$  or  $\text{Cl}^-$ ,  $n = 0$  or  $1$ ) would likely lose one R radical or anion to the solvent or another competitive acceptor to generate the neutral CH<sub>3</sub>HgR species. To approximate this process, we considered subsequent transfer of CH<sub>3</sub>S/Cl from the methylated Hg(II) complexes to the Co center in the Co-corrin-ligand models (Scheme 2) and computed gaseous and aqueous phase ligand exchange free energies.<sup>69</sup> The neutral reactant and products states for the CH<sub>3</sub>/CH<sub>3</sub>S ligand exchange are independent of the nature of the methyl transfer (heterolytic versus homolytic). The gas-phase CH<sub>3</sub>/CH<sub>3</sub>S ligand exchange free energy for the Cys thiolate ligand complex was computed to be exergonic by 11.3 kcal mol<sup>-1</sup> (Reaction I), and 3.5 kcal mol<sup>-1</sup> less favorable for the His complex (Reaction J). The corresponding CH<sub>3</sub>/Cl exchanges were even more exergonic by ~10 kcal mol<sup>-1</sup>, with  $\Delta G_{\text{r, gas}}^{\circ}$  for Reaction K = -21.2 kcal mol<sup>-1</sup> (Table 3 and Figure 2). As expected on the basis of the overall charge neutrality in both the reactants and products for ligand exchange, solvation effects are minimal, decreasing the favorability of Reactions I–L by no more than 4.0 kcal mol<sup>-1</sup> relative to the gas-phase free energy values. Thus, the current calculations predict that the corresponding differences in ligand affinity (i.e., Co–CH<sub>3</sub> and Hg–R versus Co–R and Hg–CH<sub>3</sub>) favor the formation of methylmercury for both processes.

## CONCLUSIONS

Our findings show that coordination of anionic lower-axial ligands to Co(III) and contributions from solvation favor transfer of a methyl carbanion over a methyl radical from CH<sub>3</sub>–Co(III)–corrin–ligand complexes to Hg(II) substrates. Under fully hydrated conditions in continuum solvent (SMD<sub>78.4</sub>), the energetics of carbanion dissociation are comparable to methyl radical dissociation, but the presence of an electrophilic Hg(II) substrate greatly increases the favorability of carbanion transfer compared to methyl radical transfer. Thus, our calculations support the proposal that the strictly conserved Cys in HgcA enhances the methylation of Hg(II). These findings may explain the apparent strong selective pressure to maintain the

strictly conserved Cys in HgcA orthologs, although a His variant of HgcA may also be capable of methyl transfer to a Hg(II) substrate if geometric perturbations are not too great.

The reaction free energies computed for carbanion transfer display a large dependence on the solvent dielectric constant due to charge separation in the product complexes. In the absence of structures for HgcA and any interacting protein partners that may be involved in substrate colocalization or charge stabilization, the electrostatic/dielectric environment for the methyl transfer reaction cannot be determined. Nevertheless, our model calculations shed light on key mechanistic aspects of the mercury methylation reaction carried out by HgcA.

## ASSOCIATED CONTENT

### Supporting Information

Supporting tables and figures, optimized geometries and energies for all molecules in this work, and complete ref 47. This material is available free of charge via the Internet at <http://pubs.acs.org>.

## AUTHOR INFORMATION

### Corresponding Author

\*E-mail: [parksjm@ornl.gov](mailto:parksjm@ornl.gov).

### Notes

The authors declare no competing financial interest.

## ACKNOWLEDGMENTS

This work was supported by Grant DE-SC0004895 from the U.S. Department of Energy (DOE), Office of Science, Office of Biological and Environmental Research, Subsurface Biogeochemical Research Program. ORNL is managed by UT-Battelle, LLC. for the U.S. DOE under contract DE-AC05-00OR22725. A portion of this research was conducted at the Center for Nanophase Materials Sciences, which is sponsored at ORNL by the Scientific User Facilities Division, Office of Basic Energy Sciences, U.S. DOE. This research used resources of the National Energy Research Scientific Computing Center (Grant m906), which is supported by the Office of Science of the U.S. DOE under Contract No. DE-AC02-05CH11231.

## REFERENCES

- (1) Morel, F. M. M.; Kraepiel, A. M. L.; Amyot, M. *Annu. Rev. Ecol. Syst.* **1998**, *29*, 543–566.
- (2) Wood, J. M.; Kennedy, F. S.; Rosen, C. G. *Nature* **1968**, *220*, 173–174.
- (3) Jensen, S.; Jernelov, A. *Nature* **1969**, *223*, 753–754.
- (4) Choi, S. C.; Bartha, R. *Appl. Environ. Microbiol.* **1993**, *59*, 290–295.
- (5) Ekstrom, E. B.; Morel, F. M. M.; Benoit, J. M. *Appl. Environ. Microbiol.* **2003**, *69*, 5414–5422.
- (6) Ekstrom, E. B.; Morel, F. M. M. *Environ. Sci. Technol.* **2008**, *42*, 93–99.

- (7) Gilmour, C. C.; Elias, D. A.; Kucken, A. M.; Brown, S. D.; Palumbo, A. V.; Schadt, C. W.; Wall, J. D. *Appl. Environ. Microbiol.* **2011**, *77*, 3938–3951.
- (8) Parks, J. M.; Johs, A.; Podar, M.; Bridou, R.; Hurt, R. A.; Smith, S. D.; Tomanicek, S. J.; Qian, Y.; Brown, S. D.; Brandt, C. C. *Science* **2013**, *339*, 1332–1335.
- (9) Yu, R. Q.; Reinfelder, J. R.; Hines, M. E.; Barkay, T. *Appl. Environ. Microbiol.* **2013**, *79*, 6325–6330.
- (10) Gilmour, C. C.; Podar, M.; Bullock, A. L.; Graham, A. M.; Brown, S.; Somenahally, A. C.; Johs, A.; Hurt, R.; Bailey, K. L.; Elias, D. *Environ. Sci. Technol.* **2013**, *47*, 11810–11820.
- (11) Matthews, R. G. *Acc. Chem. Res.* **2001**, *34*, 681–689.
- (12) Banerjee, R.; Ragsdale, S. W. *Annu. Rev. Biochem.* **2003**, *72*, 209–247.
- (13) Brown, K. L. *Chem. Rev.* **2005**, *105*, 2075–2150.
- (14) DeSimone, R.; Penley, M.; Charbonneau, L.; Smith, S.; Wood, J.; Hill, H.; Pratt, J.; Ridsdale, S.; Williams, R. *Biochim. Biophys. Acta* **1973**, *304*, 851–863.
- (15) Wood, J. M. *Science* **1974**, *183*, 1049–1052.
- (16) Matthews, R. G. *Met. Ions Life Sci.* **2009**, *6*, 53–114.
- (17) Svetlitchnaia, T.; Svetlitchnyi, V.; Meyer, O.; Dobbek, H. *Proc. Natl. Acad. Sci. U. S. A.* **2006**, *103*, 14331–14336.
- (18) Bertilsson, L.; Neujahr, H. Y. *Biochemistry* **1971**, *10*, 2805–2808.
- (19) Imura, N.; Sukegawa, E.; Pan, S. K.; Nagao, K.; Kim, J. Y.; Kwan, T.; Ukita, T. *Science* **1971**, *172*, 1248–1249.
- (20) Schrauzer, G. N.; Weber, J. H.; Beckham, T.; Ho, R. *Tetrahedron Lett.* **1971**, *12*, 275–277.
- (21) Schrauzer, G. N.; Seck, J. A.; Holland, R. J.; Beckham, T. M.; Rubin, E. M.; Sibert, J. W. *Bioinorg. Chem.* **1973**, *2*, 93–124.
- (22) Schrauzer, G. N.; Sibert, J. W. *J. Am. Chem. Soc.* **1970**, *92*, 3509–3510.
- (23) Dolker, N.; Maseras, F.; Lledos, A. J. *Phys. Chem. B* **2001**, *105*, 7564–7571.
- (24) Kuta, J.; Patchkovskii, S.; Zgierski, M. Z.; Kozlowski, P. M. *J. Comput. Chem.* **2006**, *27*, 1429–1437.
- (25) Kozlowski, P. M.; Kumar, M.; Piecuch, P.; Li, W.; Bauman, N. P.; Hansen, J. A.; Lodowski, P.; Jaworska, M. *J. Chem. Theory Comput.* **2012**, *8*, 1870–1894.
- (26) Hirao, H. *J. Phys. Chem. A* **2011**, *115*, 9308–9313.
- (27) Jensen, K. P.; Ryde, U. *Coord. Chem. Rev.* **2009**, *253*, 769–778.
- (28) Jensen, K. P.; Ryde, U. *J. Phys. Chem. A* **2003**, *107*, 7539–7545.
- (29) Jensen, K. P.; Ryde, U. *J. Am. Chem. Soc.* **2003**, *125*, 13970–13971.
- (30) Jensen, K. P.; Ryde, U. *J. Mol. Struct. THEOCHEM* **2002**, *585*, 239–255.
- (31) Govender, P.; Navizet, I.; Perry, C. B.; Marques, H. M. *J. Phys. Chem. A* **2013**, *117*, 3057–3068.
- (32) Andruniow, T.; Zgierski, M. Z.; Kozlowski, P. M. *J. Am. Chem. Soc.* **2001**, *123*, 2679–2680.
- (33) Kozlowski, P. M.; Kuta, J.; Galezowski, W. *J. Phys. Chem. B* **2007**, *111*, 7638–7645.
- (34) Ryde, U.; Mata, R. A.; Grimme, S. *Dalton Trans.* **2011**, *40*, 11176–11183.
- (35) Park, K.; Brunold, T. C. *J. Phys. Chem. B* **2013**, *117*, 5397–5410.
- (36) Reig, A. J.; Conrad, K. S.; Brunold, T. C. *Inorg. Chem.* **2012**, *51*, 2867–2879.
- (37) Navizet, I.; Perry, C. B.; Govender, P. P.; Marques, H. M. *J. Phys. Chem. B* **2012**, *116*, 8836–8845.
- (38) Eisenberg, A. S.; Likhtina, I. V.; Znamenskiy, V. S.; Birke, R. L. *J. Phys. Chem. A* **2012**, *116*, 6851–6869.
- (39) Conrad, K. S.; Brunold, T. C. *Inorg. Chem.* **2011**, *50*, 8755–8766.
- (40) Brunold, T. C. In *Encyclopedia of Inorganic and Bioinorganic Chemistry*; John Wiley & Sons, Ltd: New York, 2011.
- (41) Liptak, M. D.; Brunold, T. C. *J. Am. Chem. Soc.* **2006**, *128*, 9144–9156.
- (42) Stich, T. A.; Brooks, A. J.; Buan, N. R.; Brunold, T. C. *J. Am. Chem. Soc.* **2003**, *125*, 5897–5914.
- (43) Stich, T. A.; Seravalli, J.; Venkatesh Rao, S.; Spiro, T. G.; Ragsdale, S. W.; Brunold, T. C. *J. Am. Chem. Soc.* **2006**, *128*, 5010–5020.
- (44) Stich, T. A.; Buan, N. R.; Brunold, T. C. *J. Am. Chem. Soc.* **2004**, *126*, 9735–9749.
- (45) Dolker, N.; Maseras, F.; Lledos, A. J. *Phys. Chem. B* **2003**, *107*, 306–315.
- (46) Valiev, M.; Bylaska, E. J.; Govind, N.; Kowalski, K.; Straatsma, T. P.; Van Dam, H. J. J.; Wang, D.; Nieplocha, J.; Apra, E.; Windus, T. L. *Comput. Phys. Commun.* **2010**, *181*, 1477–1489.
- (47) Frisch, M. J. et al. *Gaussian 09, Revision B.01*; Gaussian, Inc.: Wallingford CT, 2009.
- (48) Perdew, J. P.; Zunger, A. *Phys. Rev. B* **1981**, *23*, 5048–5079.
- (49) Becke, A. D. *J. Chem. Phys.* **1986**, *84*, 4524–4529.
- (50) Perdew, J. P. *Phys. Rev. B* **1986**, *33*, 8822–8824.
- (51) Andruniow, T.; Zgierski, M. Z.; Kozlowski, P. M. *J. Am. Chem. Soc.* **2001**, *123*, 2679–2680.
- (52) Siegbahn, P. E. M.; Blomberg, M. R. A.; Chen, S. L. *J. Chem. Theory Comput.* **2010**, *6*, 2040–2044.
- (53) Andrae, D.; Häußermann, U.; Dolg, M.; Stoll, H.; Preuß, H. *Theor. Chim. Acta* **1990**, *77*, 123–141.
- (54) Parks, J. M.; Guo, H.; Momany, C.; Liang, L. Y.; Miller, S. M.; Summers, A. O.; Smith, J. C. *J. Am. Chem. Soc.* **2009**, *131*, 13278–13285.
- (55) Riccardi, D.; Guo, H. B.; Parks, J. M.; Gu, B. H.; Liang, L. Y.; Smith, J. C. *J. Chem. Theory Comput.* **2013**, *9*, 555–569.
- (56) Riccardi, D.; Guo, H.-B.; Parks, J. M.; Gu, B.; Summers, A. O.; Miller, S. M.; Liang, L.; Smith, J. C. *J. Phys. Chem. Lett.* **2013**, *2317*–2322.
- (57) Motreff, N.; Le Gac, S.; Luhmer, M.; Furet, E.; Halet, J. F.; Roisnel, T.; Boitrel, B. *Angew. Chem. Int. Edit.* **2011**, *50*, 1560–1564.
- (58) Grimme, S.; Antony, J.; Ehrlich, S.; Krieg, H. *J. Chem. Phys.* **2010**, *132*, 154104.
- (59) Grimme, S.; Ehrlich, S.; Goerigk, L. *J. Comput. Chem.* **2011**, *32*, 1456–1465.
- (60) <http://www.thch.uni-bonn.de/tc/DFTD3>.
- (61) Marenich, A. V.; Cramer, C. J.; Truhlar, D. G. *J. Phys. Chem. B* **2009**, *113*, 6378–6396.
- (62) Boys, S. F.; Bernardi, F. *Mol. Phys.* **1970**, *19*, 553–566.
- (63) Ragsdale, S.; Lindahl, P.; Münck, E. *J. Biol. Chem.* **1987**, *262*, 14289–14297.
- (64) Colombo, M. J.; Ha, J.; Reinfelder, J. R.; Barkay, T.; Yee, N. *Geochim. Cosmochim. Acta* **2013**, *112*, 166–177.
- (65) Holm, R. H.; Kennepohl, P.; Solomon, E. I. *Chem. Rev.* **1996**, *96*, 2239–2314.
- (66) Andruniow, T.; Zgierski, M. Z.; Kozlowski, P. M. *J. Phys. Chem. B* **2000**, *104*, 10921–10927.
- (67) Jensen, K. P.; Sauer, S. P. A.; Liljefors, T.; Norrby, P.-O. *Organometallics* **2001**, *20*, 550–556.
- (68) Pratt, D. A.; van der Donk, W. A. *J. Am. Chem. Soc.* **2005**, *127*, 384–396.
- (69) The products of CH<sub>3</sub>/SCH<sub>3</sub> ligand exchange resemble naturally occurring glutathionylcobalamin. In aqueous media, Co–Cl coordination is weak and is not expected to be physiologically relevant.

#### NOTE ADDED AFTER ASAP PUBLICATION

This paper published ASAP on December 30, 2013. The Abstract graphic was corrected and the revised version was reposted on January 6, 2014.